



Contents lists available at ScienceDirect

## International Journal of Coal Geology

journal homepage: [www.elsevier.com/locate/ijcoalgeo](http://www.elsevier.com/locate/ijcoalgeo)

## Permeability evolution of fluid-infiltrated coal containing discrete fractures

Ghazal Izadi<sup>a,\*</sup>, Shugang Wang<sup>a</sup>, Derek Elsworth<sup>a</sup>, Jishan Liu<sup>b</sup>, Yu Wu<sup>b</sup>, Denis Pone<sup>c</sup><sup>a</sup> Energy and Mineral Engineering and G3 Center, Pennsylvania State University, University Park, PA 16802, USA<sup>b</sup> Mechanical Engineering and Petroleum Engineering Program, University of Western Australia, Nedlands, Australia<sup>c</sup> ConocoPhillips, Bartlesville, Oklahoma, USA

## ARTICLE INFO

## Article history:

Received 30 July 2010

Received in revised form 13 October 2010

Accepted 13 October 2010

Available online 27 October 2010

## Keywords:

Permeability evolution of coal

Coal porosity

Swelling-induced deformation in coal

CO<sub>2</sub> geological sequestration

## ABSTRACT

We explore the conundrum of how permeability of coal decreases with swelling-induced sorption of a sorbing gas, such as CO<sub>2</sub>. We show that for free swelling of an unconstrained homogeneous medium where free swelling scales with gas pressure then porosity must increase as pressure increases. The volume change is in the same sense as volume changes driven by effective stresses and hence permeability must increase with swelling. An alternative model is one where voids within a linear solid are surrounded by a damage zone. In the damage zone the Langmuir swelling coefficient decreases outwards from the wall and the modulus increases outwards from the wall. In each case this is presumed to result from micro-fracturing-induced damage occurring during formation of the cleats. We use this model to explore anticipated changes in porosity and permeability that accompany gas sorption under conditions of constant applied stress and for increments of applied gas pressure. This model replicates all important aspects of the observed evolution of permeability with pressure. As gas pressure is increased, permeability initially reduces as the material in the wall swells and this swelling is constrained by the far-field modulus. As the peak Langmuir strain is approached, the decrease in permeability halts and permeability increases linearly with pressure. This behavior is apparent even as the constraint on damage around is relaxed and ultimately removed to represent a homogeneous linear solid containing multiple interacting flaws. In either case the rate of permeability loss is controlled by crack geometry, the Langmuir swelling coefficient and the void “stiffness” and the rate of permeability increase is controlled by crack geometry and void “stiffness” alone. Permeability evolution may be approximated by a single non-dimensional variable incorporating fracture spacing, flaw-length, Langmuir strain and initial permeability. This model represents the principal features of permeability evolution in swelling media and is a mechanistically consistent and plausible model for behavior.

© 2010 Elsevier B.V. All rights reserved.

## 1. Introduction

Injection of CO<sub>2</sub> (or other gases) into a coal seam may be used to increase the recovery of methane from the seam by preferential sorption and competitive desorption. This process is referred to as Enhanced Coal Bed Methane (ECBM) recovery. We explore how permeability of coal decreases with swelling-inducing sorption of a sorbing gas, such as CO<sub>2</sub>. We show that for free swelling of an unconstrained homogeneous medium where free swelling scales with gas pressure then porosity must increase as pressure increases. The volume change is in the same sense as volume changes driven by effective stresses and hence permeability must increase with swelling.

However, results from field and laboratory experiments indicate that coal permeability can change significantly with the sorption of gas (Mazumder and Wolf, 2008; Pini et al., 2009; Siriwardane et al., 2009; Wang et al., 2010). This is controlled by at least two

mechanisms: (1) gas pressure increase, which tends to mechanically dilate coal cleats (fractures) and thus enhance coal permeability; and (2) adsorption of CO<sub>2</sub> into coals, which induces swelling in the coal matrix (volumetric strain) and apparently reduces coal permeability by closing fracture (cleat) apertures. A number of models attempt to account for the mechanisms mentioned above (Bai et al., 1993; Cui and Bustin, 2005; Cui et al., 2007; Elsworth and Bai, 1992; Harpalani and Zhao, 1989; Zhao et al., 1994). Sawyer et al. (1990) proposed a model assuming that fracture porosity (to which permeability can be directly related) is a linear function of changes in gas pressure and concentration. A recent discussion of this model was provided by Pekot and Reeves (2003). Seidle and Huitt (1995) developed a permeability model by considering the effects of coal matrix swelling/shrinkage only, ignoring the impact of coal compressibility. Palmer and Mansoori (1998) describe a permeability model incorporating the combined effect of the elastic properties of coal and gas sorption on the resulting matrix strain. It includes a permeability loss term due to an increase in effective stress, and a permeability gain term resulting from matrix shrinkage as gas desorbs from the coal (Palmer and Mansoori, 1998). Robertson and Christiansen (2008) developed a

\* Corresponding author. Tel.: +1 814 777 4099.  
E-mail address: [gui2@psu.edu](mailto:gui2@psu.edu) (G. Izadi).

permeability model for coal and other fractured sorptive-elastic media. Their model mainly deals with variable stress conditions commonly used during measurement of permeability in the laboratory (Robertson and Christiansen, 2008).

Despite the broad range of these models there remain some issues have not been fully considered. In all of these models, the interaction between fractures and coal matrix during coal deformation is not considered. Because coal matrix and cleats have different mechanical properties, this interaction can have a significant effect on permeability changes under certain conditions. The previously discussed permeability models also assume that a change in the length of a matrix block (swelling or shrinkage) causes an equal but opposite change in the fracture aperture. However, this is not consistent with some experimental observations indicating that only a fraction of sorption-induced strain (swelling or shrinkage) contributes to fracture aperture change under certain stress conditions (Liu and Rutqvist, 2010; Liu et al., 2009; Nur and Byerlee, 1971). The effects of this mismatch between bulk deformation and fracture deformation has been identified previously for fractured rocks (Liu et al., 1999a,b, 2000) and recently for fractured coals with sorption. Despite this variety of models, none are able to replicate decreases in permeability that accompany competitive sorption under invariant stresses. This problem has been attempted by Liu et al. (2009) using a distribution of fictitious stresses within the medium. We approach this same problem by first demonstrating that in an elastic medium containing swelling constituents the relative change in pore volume is of the same sense and in the same proportion to the change in bulk volume. Thus for unconstrained swelling, both pore volume and hence permeability should increase, despite experimental observations to the contrary. To address this inconsistency, we explore the response of a model representing coal with cleats as a cracked medium containing a zone of damage close to the cleat and also absent this zone of damage. We then relax this assumption and show that this behavior may still be recovered.

## 2. Governing equations

We idealize the behavior of coal as the response of a dual porosity medium. This model considers the contribution of matrix swelling/shrinkage to changes in fracture aperture. Gas transport is understood as two hydrodynamic mechanisms by accommodating the dual-porous nature of the medium: laminar flow through the macroscopic cleat (Darcy's law) and diffusion through the coal matrix bounded by cleats (Fick's law). Fig. 1 shows how sorption- or desorption-induced strain of the coal matrix can change the porosity and the permeability

of the coal seam. The change in pore pressure changes effective stress and results in deformation. Similarly, sorption of gas into the coal matrix changes volume of the matrix and results in swelling. The governing equations for the behavior of a dual porosity medium are reported in the following section. These field equations will be coupled through a new permeability model for coal matrix and fractures.

These derivations are based on the following assumptions:

- Coal is a homogenous, isotropic and elastic continuum.
- Strain is infinitesimal.
- Gas contained within the pores is ideal and viscosity is constant under isothermal conditions.
- Coal is saturated by gas.
- The rate of gas flow through the coal is defined by Darcy's law.

In the following derivations, the width of the matrix block, the fracture width and fracture aperture are represented by  $s$ ,  $a$  and  $b$  respectively.

### 2.1. Coal seam deformation

The strain-displacement relationship is defined as:

$$\epsilon_{ij} = \frac{1}{2}(\mu_{i,j} + \mu_{j,i}) \quad (1)$$

Mechanical equilibrium of the solid phase is governed by the balance of linear momentum.

$$\sigma_{ij,j} + f_i = 0 \quad (2)$$

The constitutive relation for the deformed coal seam becomes

$$\epsilon_{ij} = \frac{1}{2G}\sigma_{ij} - \left(\frac{1}{6G} - \frac{1}{9K}\right)\sigma_{kk}\delta_{ij} + \frac{a}{3K}p_m\delta_{ij} + \frac{\beta}{3K}p_f\delta_{ij} + \frac{\epsilon_s}{3}\delta_{ij} \quad (3)$$

The elastic parameters for Eq. (3) can be written as

$$C_1 = \frac{1}{E} \quad (4)$$

$$C_2 = \frac{1}{K_n \cdot s} \quad (5)$$

$$D = \frac{1}{C_1 + C_2} \quad (6)$$

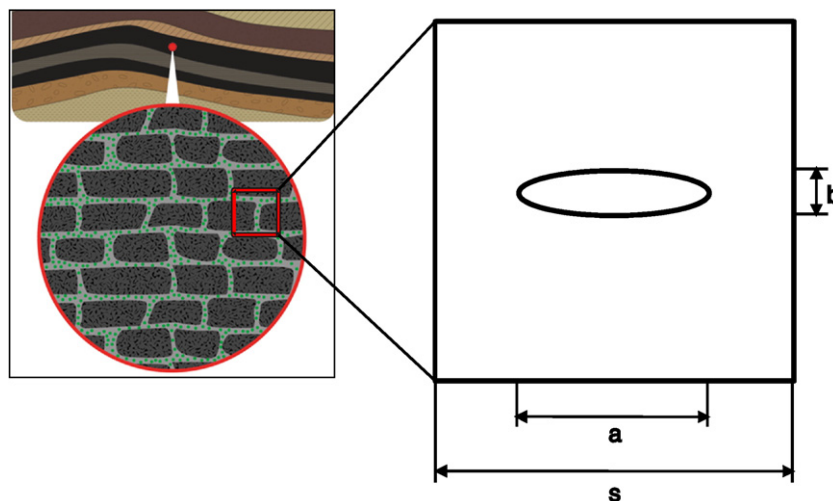


Fig. 1. Dual-porosity fractured medium.

$$G = \frac{D}{2(1 + \nu)} \quad (7)$$

$$K = \frac{D}{3(1-2\nu)} \quad (8)$$

$$\beta = 1 - \frac{K}{K_n \cdot s} \quad (9)$$

From Eqs. (1)–(3), we obtain:

$$G u_{i,kk} + \frac{G}{1-2\nu} u_{k,ki} - \alpha p_{m,i} - \beta p_{f,i} - K \varepsilon_{s,i} + f_i = 0. \quad (10)$$

Eq. (10) is the governing equation for coal deformation, where the gas pressure  $p$ , can be recovered independently from the gas flow equation as discussed following.

### 2.2. Effect of matrix swelling on fracture permeability

The permeability of coal may be defined through the cubic law for fracture permeability as

$$k = \frac{b^3}{12s} \quad (11)$$

enabling aperture to be defined as

$$b_0 = \sqrt[3]{12k_0s}. \quad (12)$$

The dynamic permeability of the cracked system may be expressed as

$$\frac{k}{k_0} = \left(1 + \frac{\Delta b}{b_0}\right)^3. \quad (13)$$

Change in aperture,  $\Delta b$ , depends on sorption-induced strain and also effective stress, when the total confining stress remains unchanged. We can define volumetric strain as

$$\varepsilon_v = \frac{\sigma_{ef}}{K} + \varepsilon_s \quad (14)$$

and the response to effective stress where total stress remains constant can be defined as

$$\sigma_{ef} = \Delta p \frac{a}{s}. \quad (15)$$

Finally, swelling to gas pressure takes the Langmuir-type form as

$$\varepsilon_s = \varepsilon_L \frac{p_m}{p_m + p_L}. \quad (16)$$

Enabling the evolution of strain to be defined as a function of matrix pressure,  $p_m$ .

In this model the swelling coefficient and modulus are defined as  $\varepsilon_L = \varepsilon_{L_0} \left(1 - \frac{E}{E_0}\right)$ ,  $E = E_0 \left(\frac{r}{a}\right)$ ,  $r = \sqrt{x^2 + y^2}$ .

### 2.3. Boundary and initial conditions

For the Navier-type equation, the displacement and stress conditions on the boundary are given as

$$u_i = \tilde{u}_i(t), \sigma_{ij} n_j = \tilde{F}_i(t) \text{ on } \partial\Omega. \quad (17)$$

where  $\tilde{u}_i(t)$  and  $\tilde{F}_i(t)$  are the components of prescribed displacement and stress on the boundary  $\partial\Omega$ , respectively and  $n_j$  is the direction cosine of the vector normal to the boundary. The initial conditions for

displacement and stress in the domain  $\Omega$  are described as

$$u_i(0) = u_{i0}, \sigma_{ij}(0) = \sigma_{ij0} \text{ in } \Omega. \quad (18)$$

For the gas flow equations, the Dirichlet and Neumann boundary conditions are defined as

$$p_m = \tilde{p}_m(t), \vec{n} \cdot \frac{k_m}{\mu} \nabla p_m = \tilde{Q}_s^f(t) \text{ on } \partial\Omega \quad (19)$$

Here,  $\tilde{p}(t)$  and  $\tilde{Q}_s(t)$  are the specified gas pressure and gas flux on the boundary. The subscript  $m$  represents matrix block respectively. The initial conditions for gas flow are

$$p_m(0) = p_{m0} \text{ in } \Omega. \quad (20)$$

## 3. Analysis of swelling-induced deformation

We approach this problem to first examine the response of a homogeneous porous continuum to determine changes in porosity that result from swelling. We then extend this to define the behavior of a non-homogeneous cracked solid with damage and then relax this assumption of damage to show that similar behavior results from a cracked medium without damage.

### 3.1. Response of a porous continuum

We consider the idealized response of a porous medium (Nur and Byerlee, 1971) where the response to swelling is added. The medium is assumed homogeneous and containing a single pore, as representative of a general porous medium Fig. 2.

We apply loads in two steps. The first step applies a uniform stress to the unperforated sample of magnitude  $P$ . The resulting volume change is

$$\frac{\Delta V_1}{V} = \frac{1}{K_s} P - \varepsilon_s \quad (21)$$

The stress throughout the unperforated sample is uniform and of magnitude,  $P$ , including the stress normal to the unperforated contour. Thus, the deformation for this loading is independent of whether the sample is perforated or not. We then apply a second stress of  $(\sigma - P)$  to the perforated sample. The resulting volume change is

$$\frac{\Delta V_2}{V} = \frac{1}{K} (\sigma - P) \quad (22)$$

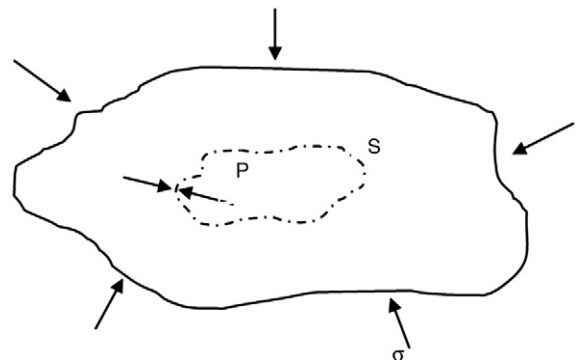


Fig. 2. A homogeneous aggregate with pore. The line S represents the surface of the pore that is subject to a pore pressure that is equal to the confining pressure.

resulting in a total overall volume change as:

$$\frac{\Delta V}{V} = \frac{\Delta V_1}{V} + \frac{\Delta V_2}{V} \quad (23)$$

corresponding to

$$\frac{\Delta V}{V} = \frac{1}{K}(\sigma - \alpha P) - \epsilon_s. \quad (24)$$

This allows the solid strain resulting from a change in fluid pressure alone to be determined as

$$\frac{\Delta V_s}{V} = (1 - \phi) \left( \frac{1}{K_s} P - \epsilon_s \right) \quad (25)$$

and consequently the change in pore space is the difference between the overall volume change and the volume change of the solid as

$$\frac{\Delta V_p}{V} = \frac{1}{K} \left[ \sigma - \left( \alpha + \frac{K}{K_s} (1 - \phi) \right) P \right] - \phi \epsilon_s \quad (26)$$

If we assume that

$$\gamma = \alpha + \frac{K}{K_s} (1 - \phi) \quad (27)$$

then finally we have the normalized pore volume change under constant total stress but with a change in pore fluid pressure and pore pressure induced swelling as

$$\frac{\Delta V_p}{V} = \frac{1}{K} (\sigma - \gamma P) - \phi \epsilon_s. \quad (28)$$

$K_s$  is the modulus of the solid,  $K$  is the bulk modulus and  $\phi$  is porosity. Correspondingly, the swelling-induced change in porosity is of the same sense as that induced by effective stresses. If pore fluid pressure is increased then porosity increases due to both the effective stresses and swelling are additive, and cannot explain the observed drop in permeability and presumed porosity seen in the unconstrained swelling of samples.

### 3.2. Response of cracked continuum with non-interacting flaws

Since a homogeneous continuum is incapable of replicating observations, we explore the response of a cracked continuum containing a zone of damage around the crack. The swelling and elastic properties will be non-homogeneous relative to the crack. We use this framework to explore the response of an idealized cleat present within the center of a fractured block as an analog for response of a fractured medium.

## 4. Model description and parameters

We choose the geometry of an elliptical fracture within a swelling medium, as shown in Fig. 2. We wish to understand how the elliptical fracture will respond under applied changes in fluid pressures when the influences of effective stresses and of swelling are separately evaluated. We consider the idealized model of Fig. 3 to represent a single fracture within a representative elemental volume. To represent conditions of invariant stresses, the sides of the model are free to deform but under invariant total stresses. Material properties are applied to the model as represented in Tables 1, 2 and 3. We represent the behavior of this geometry where fluid pressures are applied first in a non-sorbing and non-swelling medium and then in a swelling medium. These cases are applied separately.

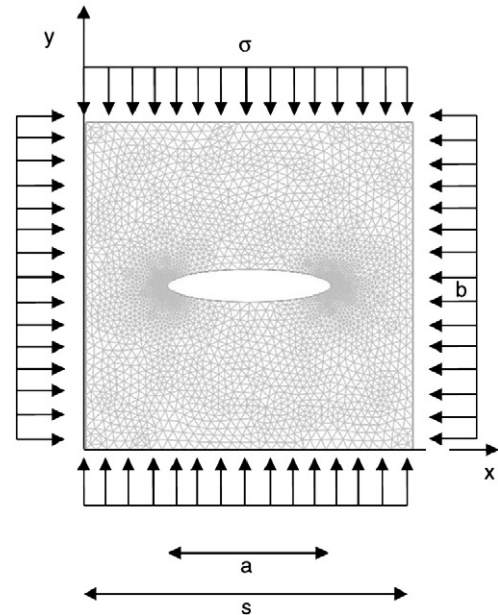


Fig. 3. Simulation model for CO<sub>2</sub> injection to a coal seam.

### 4.1. Effective stress response

We first apply a uniform fluid pressure to the elliptical fracture embedded within a solid and measure the resulting deformation of the void. Constant total stresses are applied to the boundary and fluid pressures are applied uniformly throughout the body. The resulting dilation of the void, in the direction of the short axis is shown in Fig. 4. The aperture increases linearly with applied fluid pressure, and the magnitude of this pressure deformation gives an effective stiffness of the fracture void.

### 4.2. Swelling response

To examine the swelling response we alter the material to include a damage zone around the void. This damage zone could be in elliptical coordinates to parallel the walls of the fracture, but in this case we use a radial distribution to approximate behavior. We select a damage zone to represent breakage in the wall region as a consequence of the formation of the fracture void. We postulate that in this zone the deformation modulus is reduced and the swelling coefficient increased. Thus the modulus increases linearly with radius from the magnitude prescribed at the void wall and the swelling coefficient decreases linearly outwards.

Table 1  
Parameters used in the simulation model.

| Symbol          | Description                          | Value                 | Units             |
|-----------------|--------------------------------------|-----------------------|-------------------|
| $E$             | Young's modulus of coal              | 2713                  | $M L^{-1} T^{-2}$ |
| $E_s$           | Young's modulus of coal grain        | 8143                  | $M L^{-1} T^{-2}$ |
| $\nu$           | Poisson's ratio of coal              | 0.339                 | –                 |
| $\rho_c$        | Density of coal                      | 1400                  | $M L^{-3}$        |
| $\rho_g$        | Density of CO <sub>2</sub>           | 0.717                 | $M L^{-3}$        |
| $\mu$           | Dynamic viscosity of CO <sub>2</sub> | $1.84 \times 10^{-5}$ | $M L^{-1} T^{-1}$ |
| $P_L$           | Langmuir pressure constant           | 6.109                 | $M L^{-1} T^{-2}$ |
| $V_L$           | Langmuir volume constant             | 0.015                 | $M^{-1} L^3$      |
| $\epsilon_{L0}$ | Reference swelling coefficient       | 0.02295               | –                 |
| $\phi_{m0}$     | Initial porosity of matrix           | 0.02                  | –                 |
| $k_{m0}$        | Initial permeability of fracture     | $10^{-14}$            | $L^2$             |
| $S$             | Width of matrix block                | $1 \times 10^{-2}$    | L                 |
| $a$             | Width of fracture                    | $0.5 \times 10^{-2}$  | L                 |
| $b$             | Initial height of aperture           | $10 \times 10^{-6}$   | L                 |
| $\sigma$        | Applied stress                       | $10 \times 10^6$      | $M L^{-1} T^{-2}$ |

**Table 2**  
Notation.

| Symbol             | Description                              | Units             |
|--------------------|--|-------------------|
| $a$                | Fracture width                           | L                 |
| $b$                | Fracture aperture                        | L                 |
| $E$                | Elastic modulus                          | $M L^{-1} T^{-2}$ |
| $f_{,i}$           | Component of body force                  | $M L^{-1} T^{-2}$ |
| $G$                | Shear modulus                            | $M L^{-1} T^{-2}$ |
| $k$                | Coal permeability                        | $L^2$             |
| $K$                | Bulk modulus                             | $M L^{-1} T^{-2}$ |
| $K_s$              | Grain bulk modulus                       | $M L^{-1} T^{-2}$ |
| $K_n$              | Normal stiffness of individual fractures | $M L^{-2} T^{-2}$ |
| $p$                | Gas pressure in matrix                   | $M L^{-1} T^{-2}$ |
| $p_a$              | Standard atmosphere pressure             | $M L^{-1} T^{-2}$ |
| $p_L$              | Langmuir pressure                        | $M L^{-1} T^{-2}$ |
| $\vec{q}_g$        | Darcy's velocity vector                  | $L T^{-1}$        |
| $S$                | Width of matrix block                    | L                 |
| $u_i$              | Component of displacement                | L                 |
| $V_L$              | Langmuir volume constant                 | $M^{-1} L^3$      |
| $\alpha, \beta$    | Biot coefficient                         | -                 |
| $\Delta b$         | Change in aperture height                | L                 |
| $\sigma_{ij}$      | Component of the total stress tensor     | $M L^{-1} T^{-2}$ |
| $\sigma_{kk}$      | Components of the mean stress            | $M L^{-1} T^{-2}$ |
| $\sigma_{ef}$      | Effective stress                         | $M L^{-1} T^{-2}$ |
| $\delta_{ij}$      | Kronecker delta                          | -                 |
| $\varepsilon_{ij}$ | Component of the total strain tensor     | -                 |
| $\varepsilon_s$    | Swelling strain                          | -                 |
| $\varepsilon_v$    | Volumetric strain                        | -                 |
| $\varepsilon_L$    | Swelling coefficient                     | -                 |
| $\mu$              | Dynamic viscosity of the gas             | $M L^{-1} T^{-1}$ |
| $\phi$             | Porosity                                 | -                 |
| $\rho_g$           | Gas density                              | $M L^{-3}$        |
| $\rho_{ga}$        | Gas density at standard conditions       | $M L^{-3}$        |

Applying a uniform pressure to the solid surrounding the elliptical void enables the influence of swelling to be determined on the change in void aperture. The resulting volumetric strain with pressure is given by Eq. (16) as a Langmuir strain. The Langmuir adsorption isotherm assumes that the gas attaches to the surface of the coal and covers the surface as a single layer of gas. Nearly all of the gas stored by adsorption in coal exists in a condensed, near liquid state. At low-pressures, this dense state allows greater volumes to be stored by sorption than is possible by compression and at high pressure swelling strains become constant. For constant void width,  $a$ , relative to the width of the enveloping block,  $s$ , the closure of the void is insensitive to the height of the void opening. This is because the high modulus around the periphery of the square block acts as a constraining ring. This forces closure of the void as the swelling of the interior proceeds, thus the void closure scales linearly with an increase in the swelling coefficient of the material, but is near constant with length of the void short axis. This linearity prevails provided the faces of the closing void do not contact. The initial aperture of the coal may be evaluated from Eq. (12). The change in aperture of the void is superposed on this initial aperture as swelling progresses. For an initial high permeability, the initial aperture,  $b_0$  will be largest, but the aperture reduction will be the same for all permeabilities, as shown in Fig. 5. Since the swelling-induced reduction in the void aperture is independent of the initial aperture, the closure may be used to evaluate final aperture and hence scaled permeability. Void opening scales according to the physical parameters controlling response and correspondingly we can define

$$\Delta b = f(E, \varepsilon_L, \alpha, P, P_L). \quad (29)$$

**Table 3**  
Coal properties.

| Mine    | Coal seam            | Location         | Depth (m) | Rank       |
|---------|----------------------|------------------|-----------|------------|
| Harmony | Northumberland Basin | Mount Carmel, PA | 122       | Anthracite |

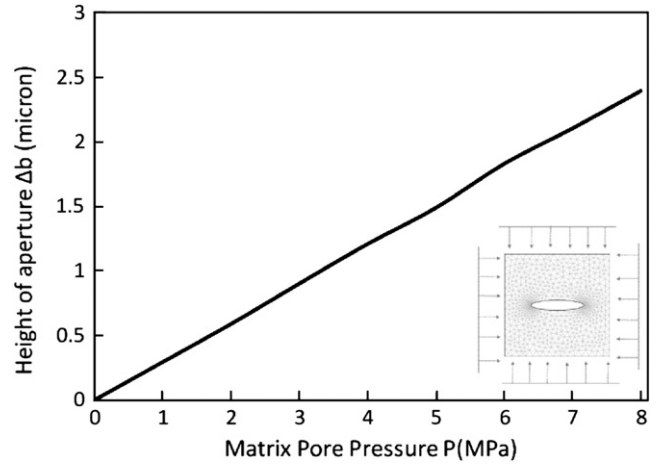


**Fig. 4.** The relation between change of aperture and matrix pore pressure by applying effective stress.

The normalized magnitude of closure is shown in Fig. 6 for a dimensionless pressure of  $(P/E)\varepsilon_L$ .

#### 4.3. Ensemble response

We combine the two deformational responses for the separate influences of effective stress and swelling. The change in void aperture with pressure due to the individual effects of swelling and of effective stresses. These two influences may be combined to determine the net change in permeability in the system. Where initial permeability is evaluated from Eq. (12) the change in permeability may be evaluated directly for a change in aperture from Eq. (13). This response is represented in Fig. 7 for initial permeabilities of  $10^{-13}$  to  $10^{-15} \text{ m}^2$ . This identifies the initial reduction in permeability caused by swelling of the unconstrained block and the subsequent influence of effective stresses alone as swelling effects halt at higher pressures. It identifies a non-linear initial decrease in permeability that reduces to a minimum magnitude, and that ultimately turns to an increase as the influence of effective stresses become dominant. This behavior replicates the response of injection experiments conducted on unconstrained coals, i.e. at constant total stress.

#### 4.4. Response of cracked continuum with interacting flaws

To determine the necessity of incorporating a damage zone we explore the response of a homogeneous medium seeded with a regular

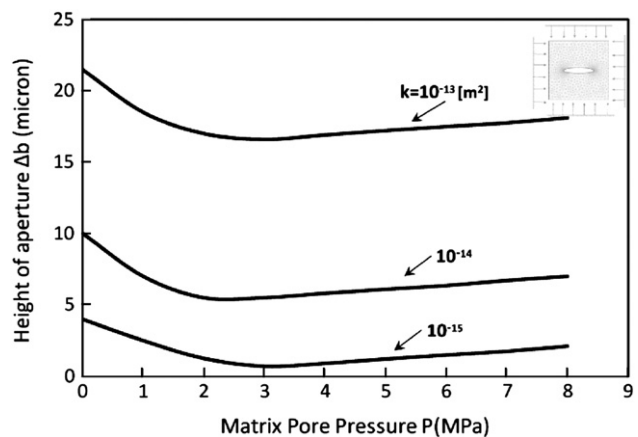


**Fig. 5.** The relation between change of aperture and matrix pore pressure.

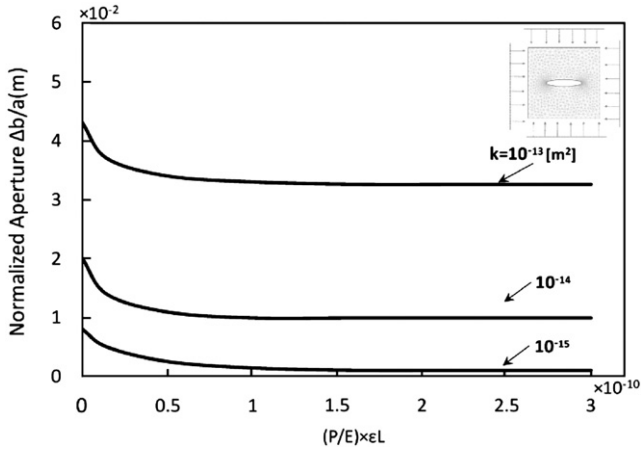


Fig. 6. The relation between ratio of aperture change to initial aperture and dimensionless pressure.

array of interacting cracks. We examine the influence of effective stress and swelling response for an elliptical crack where the deformation modulus and swelling coefficient are constant with radius.

We consider two models to represent this behavior. The first is a single component part removed from the array where the appropriate boundary conditions are for uniform displacement along the boundaries. This represents the symmetry of the displacement boundary condition mid-way between flaws as shown in Fig. 8.A. An alternative method to represent this geometry is an equivalent model that incorporates multiple flaws and automatically accommodates the appropriate displacement boundary condition as shown in Fig. 8.B.

We repeat the prior analysis to examine the change in aperture due to the combined influence of swelling and effective stress. For each of the two representations of an interacting network of flaws the evolution of aperture is identical as apparent in Fig. 9.A and B and conforms to the anticipated behavior where swelling effects are staunched at higher gas pressures. Similarly, where these changes in apertures are converted to permeabilities, identical permeability evolution trends result for the two models. These responses are represented in Fig. 9.C and D for initial permeabilities of  $10^{-13}$  to  $10^{-15}$  m<sup>2</sup>.

#### 4.5. Generalized response

We generalize our understanding of the reduction of permeability due to unconstrained swelling and the subsequent influence of effective stresses alone as swelling effects halt at higher pressures. We

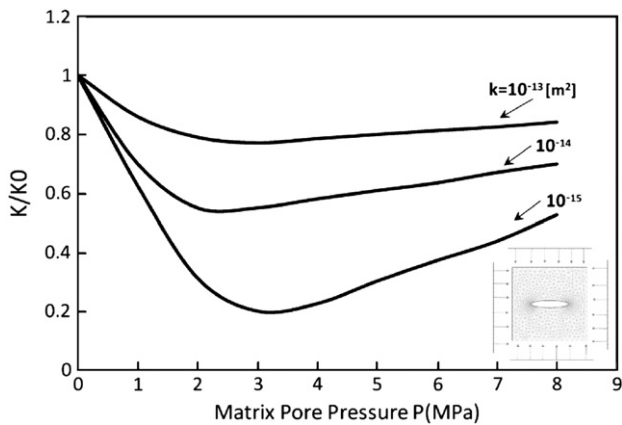


Fig. 7. The relation between fracture permeability ratio and matrix pore pressure.

generalize changes in porosity and permeability that accompany gas sorption under conditions of constant applied stress and for increments of applied gas pressure for fractures. Specifically we explore the relation between the reduction of permeability by applying swelling-induced sorption of a sorbing gas and the increase of permeability due to the influence of effective stress for a generalized geometry. We describe the response of a cracked continuum with various fracture sizes for idealized fracture widths.

We consider different ratios of the fracture length to matrix block size, defined as the fracture spacing. This ratio changes from 0.025 to 1, the normalized magnitude of closure is shown in Fig. 10.A for a dimensionless pressure of  $(P/E)\epsilon_L$ . The initial reduction in permeability caused by swelling of the unconstrained block and ultimate increase in permeability under the influence of effective stress is shown in Fig. 10.B, where initial permeability is  $10^{-13}$  m<sup>2</sup>.

The response may be further generalized in considering an approximation of the true mechanical behavior. This is to accommodate the swelling of a soft medium (vanishing modulus) that is constrained within a rigid outer shell. This geometry contains a fracture of width,  $a$ , spacing between fractures,  $s$ , and initial aperture,  $b$ .

Total volume  $V$  for rectangular crack is defined as

$$V = s^3. \quad (30)$$

The corresponding change in volume,  $\Delta V$  is defined as

$$\Delta V = s^3 \epsilon_s. \quad (31)$$

The change in volume of the fracture,  $\Delta V_f$ , depends on the length and width of fracture and also the size of the matrix when the external displacement of the body is null. Thus the volumetric change in the fracture is defined as

$$\Delta V_f = a.s.\Delta b. \quad (32)$$

Substituting Eq. (30) into (31) and equating the result with Eq. (32) yields

$$V\epsilon_s = a.s.\Delta b. \quad (33)$$

Where the external boundary has zero displacement, the swelling strain is defined as

$$\epsilon_s = \frac{\Delta b.a}{s.s} \quad (34)$$

and also the resulting change in aperture may be recovered by substituting the strain of Eq. (34) into the volume constraint relationship of Eq. (33) as

$$\Delta b = \frac{\epsilon_s s^2}{a}. \quad (35)$$

Finally, from Eq. (35) we can determine

$$\frac{\Delta b}{b_0} = \frac{\epsilon_s s^2}{ab_0}. \quad (36)$$

Where initial aperture is evaluated from Eq. (12) and the change in permeability is defined in Eq. (13) we can recover

$$\frac{k}{k_0} = \left(1 + \frac{\epsilon_s s^2}{ab_0}\right)^3 = \left(1 + \left(\frac{\epsilon_L s^2}{ab_0}\right) \frac{p}{p_m + p_L}\right)^3. \quad (37)$$

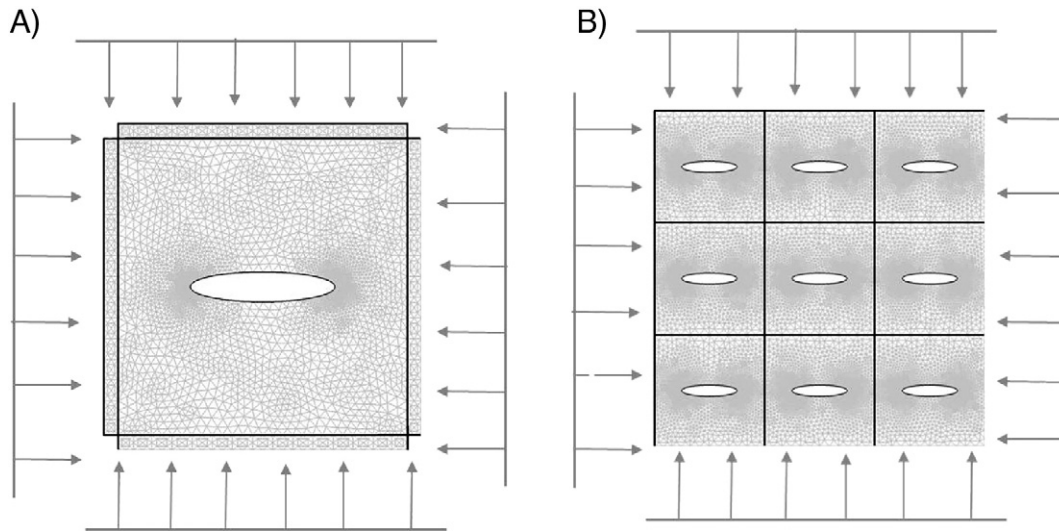


Fig. 8. Simulation model.

Thus, permeability scales according to the physical parameters controlling response as

$$\frac{k}{k_0} = f\left(\frac{\varepsilon_L s^2}{ab_0}; p; p_L\right). \quad (38)$$

This enables the evolution of relative permeabilities to be determined as a function of the non-dimensional parameter  $s_n'$

incorporating initial permeability, swelling strain and geometric constraints, alone as

$$s_n' = \frac{\varepsilon_L s^2}{a\sqrt[3]{12k_0s}}. \quad (39)$$

This relation is used to represent the families of permeability evolution for constant magnitudes of  $s_n'$ . The resulting permeability

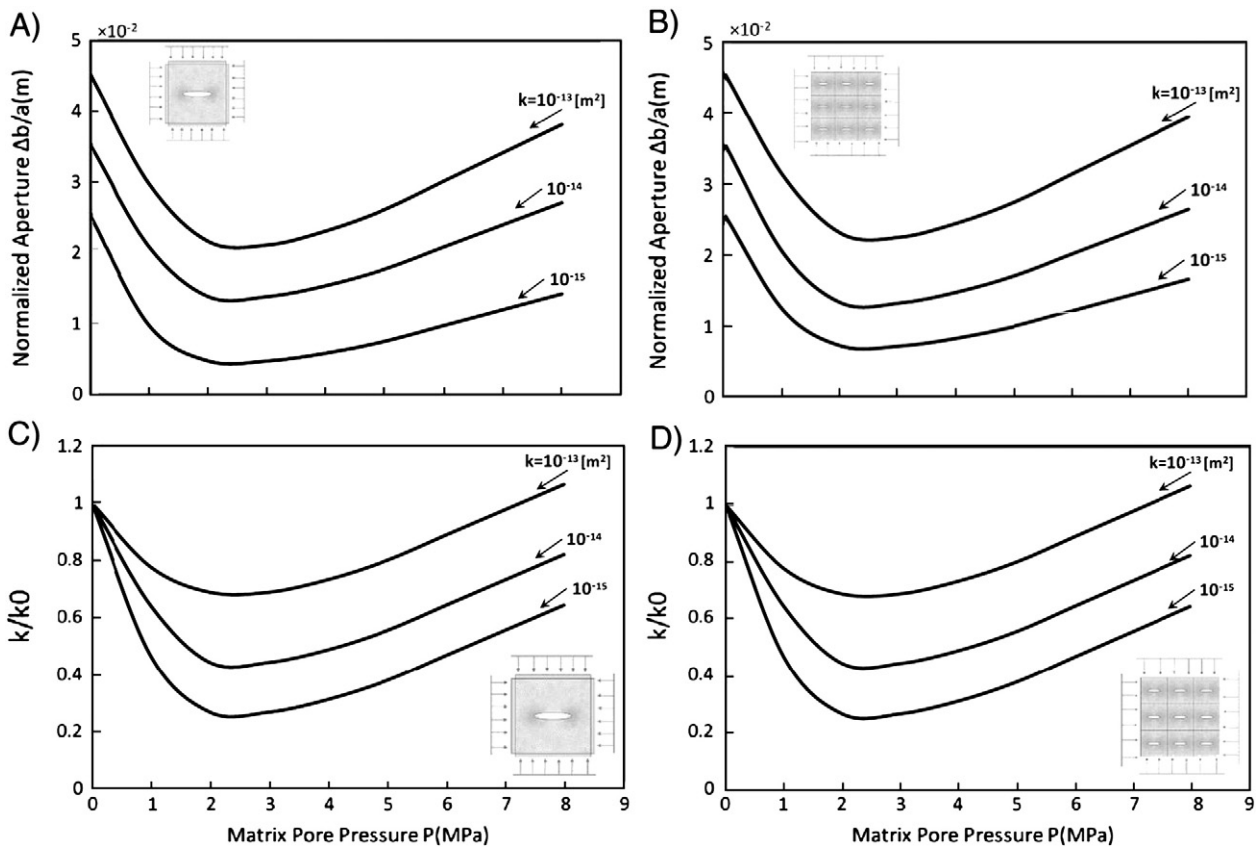


Fig. 9. A) The relation between ratio of aperture change to initial aperture and pressure for one fracture. B) The relation between ratio of aperture change to initial aperture and pressure for multiple fractures. C) The relation between matrix permeability ratio and matrix pore pressure for one fracture. D) The relation between matrix permeability ratio and matrix pore pressure for multiple fractures.

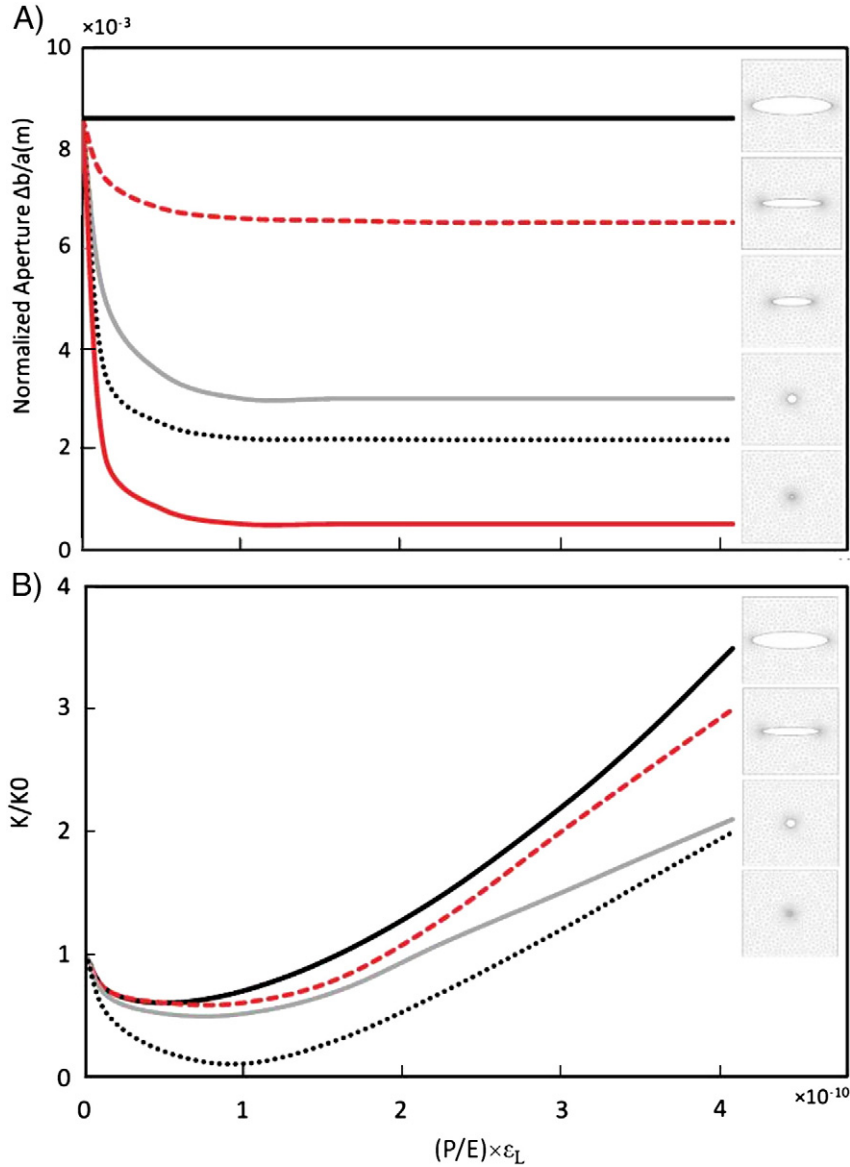


Fig. 10. A) The relationship between the ratio of aperture change and dimensionless pressure. B) The relationship between matrix permeability ratio and dimensionless pressure.

evolution for different initial permeabilities of  $10^{-13}$  to  $10^{-15}$  m<sup>2</sup> is shown as a function of dimensionless pressure ( $p/p_L$ ) in Fig. 11.

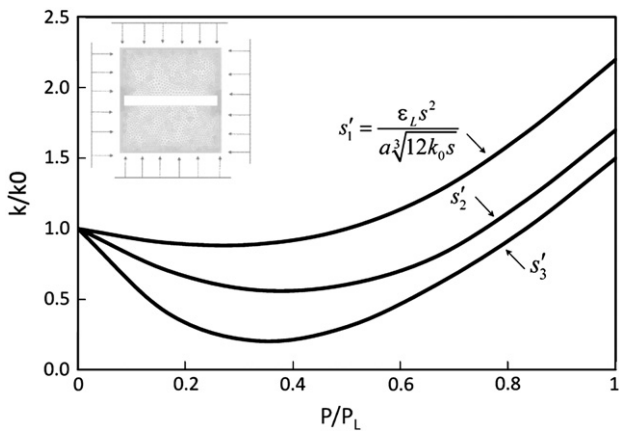


Fig. 11. The relationship between fracture permeability ratio and dimensionless pressure.

### 5. Experimental observations

We contrast the response of coal containing multiple interacting flaws with that for a fully cracked medium to explore the veracity of this proposed model for permeability evolution due to swelling. This behavior is investigated experimentally. The simplest test of this mechanistic model is to examine the evolution of permeability in samples containing multiple embedded cracks with permeability evolution where the fracture completely cleaves the sample. Presence of low-pressure permeability reduction in the former (i) and absence in the latter (ii) will suggest that our model may be correct. Descriptions of experimental investigations follow:

This Experiment was completed in a Temco triaxial core holder capable of accepting membrane-sheathed cylindrical samples (2.5 cm diameter × 5 cm long) and loaded independently in the radial and axial directions. Confining and axial stresses to 35 MPa are applied by a dual cylinder ISCO pump with control to ±0.007 MPa. Axial strain is measured by a linear variable displacement transducer (LVDT, Trans-Tek 0244) and volumetric strain is measured by volume change in the confining fluid. Upstream and downstream fluid pressures are measured by pressure transducers (PDCR 610 and Omega PX302-5KGV).

The cylindrical sample is sandwiched within the Temco cell between two cylindrical stainless steel loading platens with through-going flow connections and flow distributors. Detailed experimental method and measurement procedure can be referenced in (Wang et al., 2010). An intact sample and a sample with a single thoroughgoing fracture (separate parts) are used and permeabilities are measured at various gas pressures for constant total stress.

Experiments are conducted with He, CH<sub>4</sub>, and CO<sub>2</sub> and at room temperature. We define effective stress as the difference between confining stress and pore pressure inside the sample (Biot coefficient of unity) for constant total stresses at 6 MPa. The influence of effective stress-driven changes in volume are examined with non-sorbing He as the permeant. Permeabilities are measured to determine the influence of adsorption and swelling on the evolution of permeability.

Permeability measured with respect to pore pressure at a constant total stress of 6 MPa for the intact sample is shown in Fig. 12. Permeability to He shows an increase in permeability with increasing pore pressure. But for the sorbing gases CH<sub>4</sub> and CO<sub>2</sub>, permeabilities first decrease as dominated by the swelling, then recover as the increase due to effective stress law outstrips the reduction induced by swelling.

The permeability evolution with respect to pore pressure at a constant total stress of 6 MPa for the split sample is shown in Fig. 13. Permeability to He shows an increase in permeability with increasing pore pressure. But for the sorbing gases CH<sub>4</sub> and CO<sub>2</sub>, which are anticipated to cause swelling, there is no permeability reduction regime at low gas pressures. This observation is congruent with the need for connected bridges to be present within the cracked continuum to cause the observed swelling-induced reduction in permeability.

## 6. Conclusions

In the previous we show that permeability reduction in unconstrained swelling cannot be explained in homogeneous systems by poromechanical arguments, alone. To the converse, where swelling is unconstrained, the porosity will grow in the same proportion as the bulk strain of the ensemble system. This infers that in swelling systems, porosity will increase and permeability would also increase. As an alternative we explore a model of structured inhomogeneity where swelling coefficient and modulus vary spatially relative to the pore. In this model, the natural constraining effect of the high modulus, remote from the void, prompts reduction in porosity with free swelling. In a system where swelling is limited by a Langmuir-type response, this swelling ultimately ceases at higher pressures and the influence of effective stresses take over. Correspondingly this model is capable of replicating observed behavior. Where the requirement for a zone of damage is relaxed, and a homogeneous medium is accommodated with multiple interacting cracks, the same features of the permeability response are recovered.

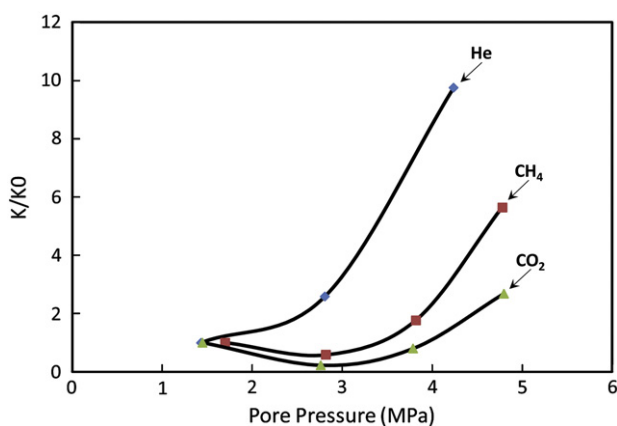


Fig. 12. The relation between permeability and pore pressure for intact sample.

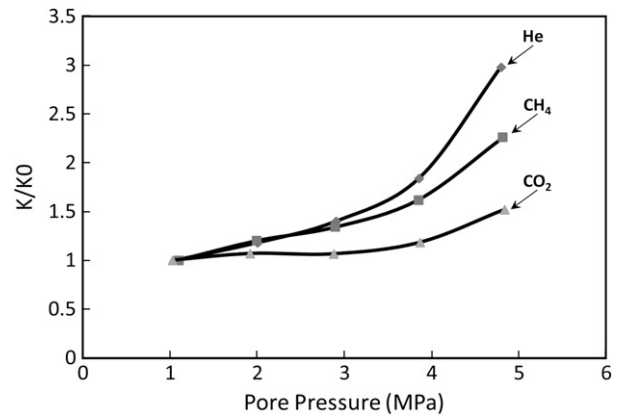


Fig. 13. The relation between permeability and pore pressure for split sample.

This behavior may also be investigated experimentally. Other experimental results for partially cracked media show the dependence of permeability on swelling. For a sorbing gas, the low-pressure response is dominated by a reduction in permeability. Where a through-going crack is present, the resulting evolution of permeability is absent the initial permeability reduction under low-pressures. This observation suggests that the presence of bridges across fractures is a crucial component in replicating this change in the sense of permeability evolution with pressure.

## Acknowledgements

This work is a partial result of support from ConocoPhillips and from NIOSH under contract 200-2008-25702. These sources of support gratefully acknowledged.

## References

- Bai, M., Elsworth, D., Roegiers, J.C., 1993. Multiporosity Multipermeability Approach to the Simulation of Naturally Fractured Reservoirs. *Water Resources Research* 1621–1633.
- Cui, X.J., Bustin, R.M., 2005. Volumetric strain associated with methane desorption and its impact on coalbed gas production from deep coal seams. *Aapg Bulletin* 89 (9), 1181–1202.
- Cui, X.J., Bustin, R.M., Chikatamarla, L., 2007. Adsorption-induced coal swelling and stress: Implications for methane production and acid gas sequestration into coal seams. *Journal of Geophysical Research-Solid Earth* 112 (B10).
- Elsworth, D., Bai, M., 1992. Flow-deformation response of dual-porosity media. *Journal of Geotechnical Engineering-ASCE* 118 (1), 107–124.
- Harpalani, S., Zhao, X., 1989. An Investigation of the Effect of Gas Desorption on Gas Permeability. *Proceedings of the Coalbed Methane Symposium*. University of Alabama, Tuscaloosa, Alabama, pp. 57–64.
- Liu, H.H., Rutqvist, J., 2010. A new coal-permeability model: internal swelling stress and fracture-matrix interaction. *Transport in Porous Media* 82 (1), 157–171.
- Liu, J., Elsworth, D., Brady, B.H., 1999a. A coupled hydromechanical system defined through rock mass classification schemes. *International Journal for Numerical and Analytical Methods in Geomechanics* 23 (15), 1945–1960.
- Liu, J., Elsworth, D., Brady, B.H., 1999b. Linking stress-dependent effective porosity and hydraulic conductivity fields to RMR. *International Journal of Rock Mechanics and Mining Sciences* 36 (5), 581–596.
- Liu, J., Elsworth, D., Brady, B.H., Muhlhaus, H.B., 2000. Strain-dependent fluid flow defined through rock mass classification schemes. *Rock Mechanics and Rock Engineering* 33 (2), 75–92.
- Liu, H.H., Rutqvist, J., Berryman, J.G., 2009. On the relationship between stress and elastic strain for porous and fractured rock. *International Journal of Rock Mechanics and Mining Sciences* 46 (2), 289–296.
- Mazumder, S., Wolf, K.H., 2008. Differential swelling and permeability change of coal in response to CO<sub>2</sub> injection for ECBM. *International Journal of Coal Geology* 74 (2), 123–138.
- Nur, A., Byerlee, J.D., 1971. Exact effective stress law for elastic deformation of rock with fluids. *Journal of Geophysical Research* 76 (26), 6414–6414.
- Palmer, I., Mansoori, J., 1998. How permeability depends on stress and pore pressure in coalbeds: a new model. *Paper SPE 52607*. SPE Reserv. Eval. Eng. *Spe Journal* 1 (6), 539–544.
- Pekot, L.J., Reeves, S.R., 2003. Modeling the effects of matrix shrinkage and differential swelling on coal methane recovery and carbon sequestration. *Paper 0328*.

- International Coalbed Methane Symposium. University of Alabama, Tuscaloosa, Alabama.
- Pini, R., Ottiger, S., Burlini, L., Storti, G., Mazzotti, M., 2009. Role of adsorption and swelling on the dynamics of gas injection in coal. *J. Geophys. Res.* 114, B04203 [doi:10.1029/2008JB005961](https://doi.org/10.1029/2008JB005961).
- Robertson, E.P., Christiansen, R.L., 2008. A permeability model for coal and other fractured, sorptive-elastic media. *Spe Journal* 13 (3), 314–324.
- Sawyer, W.K., Paul, G.W., Schraufnagel, R.A., 1990. Development and application of a 3D coalbed simulator. Paper CIM/SPE 90-1119. International Technical Meeting Hosted Jointly by the Petroleum Society of CIM and the Society of Petroleum Engineers, Calgary, Alberta, Canada.
- Seidle, J.P., Huitt, L.G., 1995. Experimental Measurement of Coal Matrix Shrinkage due to Gas Desorption and Implications for Cleat Permeability Increases. Paper SPE 30010. Proceedings of SPE International Meeting on Petroleum Engineering, Beijing, China.
- Siriwardane, H., et al., 2009. Influence of carbon dioxide on coal permeability determined by pressure transient methods. *International Journal of Coal Geology* 77 (1–2), 109–118.
- Wang, S., Elsworth, D., Liu, J., 2010. Evolution of Permeability in Coal to Sorbing Gases – A Preliminary Study. 44th U.S. Rock Mechanics Symposium. July 2010, Salt Lake City, Utah, 2009.
- Zhao, C.B., Xu, T.P., Valliappan, S., 1994. Numerical modeling of mass-transport problems in porous-media – a review. *Computers & Structures* 53 (4), 849–860.